Paramagnetic fluctuations in $Pr_{0.65}Ca_{0.35}MnO_3$ around the charge-ordering temperature



2006 J. Phys.: Condens. Matter 18 1509

(http://iopscience.iop.org/0953-8984/18/5/003)

INSTITUTE OF PHYSICS PUBLISHING JOURNAL OF PHYSICS: CONDENSED MATTER

J. Phys.: Condens. Matter **18** (2006) 1509–1517 doi:10.1088/0953-8984/18/5/003

# Paramagnetic fluctuations in $Pr_{0.65}Ca_{0.35}MnO_3$ around the charge-ordering temperature

**A Daoud-Aladine[1,5], B Roessli[2], S N Gvasaliya[2], C Perca[3], L Pinsard-Gaudart[3], J Rodrìguez-Carvajal[4] and A Revcolevschi[3]**

[1] ISIS Department, Rutherford Appleton Laboratories, Chilton, Didcot, Oxfordshire OX11 0QX, UK
[2] Laboratory for Neutron Scattering ETH Zurich and Paul Scherrer Institut, CH-5232 Villigen, Switzerland
[3] Laboratoire de Physico-Chimie de l'Etat Solide, Université Paris Sud, Bâtiment 414, 91405 Orsay, France
[4] Laboratoire Léon Brillouin, CEA-CNRS Saclay, 91191 Gif sur Yvette, France

E-mail: A.Daoud-Aladine@rl.ac.uk

Received 16 August 2005
Published 17 January 2006
Online at stacks.iop.org/JPhysCM/18/1509

**Abstract**

We have studied the ferromagnetic and antiferromagnetic fluctuations in the charge-ordered $Pr_{0.65}Ca_{0.35}MnO_3$ antiferromagnet by triple-axis neutron spectrometry. Whereas ferromagnetic fluctuations are observed above and below the charge-ordering transition ($T_{CO}$), the antiferromagnetic fluctuations develop only below $T_{CO}$. The dynamical exponent $z$ of both ferromagnetic and antiferromagnetic fluctuations are determined. The ferromagnetic fluctuations are not completely suppressed below $T_{CO}$ and their correlation lengths are short-ranged at all temperatures. The results are discussed with respect to the Zener polaron model recently introduced to describe the charge-ordered state of $Pr_{0.6}Ca_{0.40}MnO_3$.

## 1. Introduction

$La_{1-x}Ca_xMnO_3$ compounds are prototype colossal magneto-resistive manganites for compositions $0.2 < x < 0.45$, i.e. they show a large increase of the electronic conductivity below ferromagnetic ordering that can be influenced by application of a magnetic field [1, 2]. The ferromagnetic transition temperature concomitant to the transition to a metallic state is highest for $x = 0.33$ [3, 4]. This is primarily thought to originate from the double-exchange ferromagnetic interaction, which induces the delocalization of the electrons at the $e_g$ level of the Mn 3d shell in a spin polarized band, as proposed by De Gennes [5, 6]. For $x > 0.5$, the $La_{1-x}Ca_xMnO_3$ compounds become insulating materials that undergo phase transitions to

[5] Author to whom any correspondence should be addressed.

charge-ordered states where all 3d electrons are localized. The charge-ordering transition is always associated to an antiferromagnetic phase transition at lower temperatures.

The physical properties of insulating manganites were given a theoretical basis by Goodenough who considered the super-exchange mechanism in conjunction with covalency between Mn and O ions and gave detailed predictions for the correlation between antiferromagnetic, charge, and orbital ordering [8]. The super-exchange picture suggests that magnetic couplings arise between ordered ions, so that $e_g$ electrons must be localized at the Mn atomic level. This supposes ionic ordering of $Mn^{4+}$ ions with empty $e_g$ levels, and $Mn^{3+}$ where the orbital degeneracy of the $e_g$ level is lifted. The appearance of superlattice reflections in the diffraction patterns below $T_{CO}$ has been taken as evidence that charge and orbital ordering is due to Jahn–Teller distortions of $Mn^{3+}O_6$ octahedra [9, 10] in the prototype charge-ordered half-doped $Ln_{0.5}Ca_{0.5}MnO_3$ (Ln: lanthanide, or Y) manganites.

$Pr_{1-x}Ca_xMnO_3$ perovskites also have a ferromagnetic ground state for $0.15 < x < 0.3$ and charge-ordered antiferromagnetic ground states at higher values of Ca-doping. However, in contrast to the La-manganites, $Pr_{1-x}Ca_xMnO_3$ compounds are insulating over the whole range of Ca-doping [10]. For compositions with $x \sim 0.3$, the transition to a ferromagnetic metallic state can be only induced by application of an external magnetic field [11]. The charge-ordered state between $0.3 < x < 0.5$ is very similar to that found in $La_{0.5}Ca_{0.5}MnO_3$ [10, 12].

The de Gennes double-exchange mechanism is supposed to be suppressed when ionic charge-ordering takes place. In contrast to these expectations, it was shown that in charge-ordered $Pr_{1-x}Ca_xMnO_3$ compounds ($0.35 < x < 0.5$), ferromagnetic fluctuations are present above $T_{CO}$ and survive down to the Néel temperature [19]. We re-investigated the spectrum of paramagnetic fluctuations in $Pr_{1-x}Ca_xMnO_3$ with $x = 0.35$ between $T_{CO} \approx 235$ K and $T_N \approx 170$ K using triple-axis neutron spectrometry to study the interplay between ferromagnetic and antiferromagnetic fluctuations. We find that the antiferromagnetic fluctuations appear at $T_{CO}$ and have a spin-stiffness exponent $z = 1.5$. The correlation length of the antiferromagnetic fluctuations becomes critical at $T_N$, whereas the ferromagnetic fluctuations are short-ranged and show a pronounced anomaly at $T_{CO}$.

## 2. Experimental and data analysis

The measurements were performed with the triple-axis spectrometer TASP at the neutron spallation source SINQ in Switzerland. The sample consists of a twinned $Pr_{0.65}Ca_{0.35}MnO_3$ single crystal with dimensions $3 \times 3 \times 10$ mm$^3$. The mosaic of the sample was less than $\eta = 1°$. The single crystal was oriented to access the (001)/(100) diffraction plane of one of the domains, which has an orthorhombic cell with cell parameters approximately $(\sqrt{2}a_p, \sqrt{2}a_p, 2a_p)$, where $a_p$ is the Mn–Mn distance of the pseudo-cubic Mn lattice. The crystal was mounted inside a closed-cycle refrigerator. The measurements were performed with a constant final neutron wavevector $k_f = 1.64$ Å and collimation $10'/k_i$–$40'$–$40'$–$80'$. With such a configuration the energy resolution at zero energy transfer is $\Delta E \approx 0.2$ meV. A PG filter was installed after the sample to remove higher-order neutron wavelengths. The spectrum of ferromagnetic fluctuations was measured near the (0, 0, 2) Bragg peak, whereas the antiferromagnetic excitations were studied in the vicinity of the (0, 0, 1) position.

The data were analysed using the following model function:

$$I(\mathbf{Q}, \omega) = S_{\text{incoh}}(\omega) + S_{\text{para}}(\mathbf{Q}, \omega) \otimes R(\mathbf{Q}, \omega) + Bck \tag{1}$$

where $S_{\text{incoh}}(\omega)$ is the $\mathbf{Q}$-independent incoherent scattering, and $S_{\text{para}}$ is the scattering function which describes the paramagnetic fluctuations around the ferromagnetic (F), respectively antiferromagnetic (AF), zone centres. The symbol $\otimes$ stands for the convolution of the scattering

function with the resolution function of the spectrometer $R(\mathbf{Q}, \omega)$, and $Bck$ is the background, which amounts to 1 neutron count $\text{min}^{-1}$. The incoherent scattering was measured at $T = 10$ K away from the Bragg position and was found to be well described by a Gaussian function with a full-width at half maximum $\sigma = 0.21$ meV.

The neutron scattering function $S(\mathbf{Q}, \omega)$ is related to the imaginary part of the dynamical susceptibility $\text{Im}\,\chi(\mathbf{Q}, \omega)$ through the fluctuation-dissipation theorem:

$$S(\mathbf{Q}, \omega) = \frac{1}{\pi}[1 - \exp(-\hbar\omega/k_B T)]^{-1}\,\text{Im}\,\chi(\mathbf{Q}, \omega). \tag{2}$$

For paramagnetic fluctuations $\text{Im}\,\chi(\mathbf{Q}, \omega)$ is usually approximated by a Lorentzian function

$$\text{Im}\,\chi(\mathbf{Q}, \omega) = C\chi(0)\frac{\kappa^2}{q^2 + \kappa^2} \times \frac{\omega\Gamma(\mathbf{q})}{\omega^2 + \Gamma^2(\mathbf{q})} \tag{3}$$

where $C$ is a normalization constant, $\chi(0)$ the static susceptibility at $\mathbf{q} = 0$, $\kappa$ is the inverse of the correlation length $\xi$ and $\Gamma(\mathbf{q})$ describes the damping of the fluctuations measured from the nearest Brillouin zone centre $\mathbf{q} = \mathbf{Q} - \tau$. To obtain the parameters $\kappa$ and $\gamma$, we performed both constant-energy and constant-$q$ scans.

## 3. Results

### *3.1. Antiferromagnetic fluctuations*

Antiferromagnetic paramagnetic fluctuations were measured close to the antiferromagnetic zone centre $\vec{\tau} = (0, 0, 1)$. Figure 1 shows constant-energy scans $\hbar\omega = 0.5$ meV along $(0, 0, 1 \pm q)$ in $Pr_{0.65}Ca_{0.35}MnO_3$. The intensity of the antiferromagnetic fluctuations decreases above $T_N$ and the line shape broadens in $q$-space, reflecting the decrease of the correlation length with increasing temperature. We fitted the data collected around the antiferromagnetic wavevector with the model function (equations (1)–(3)). The results of the calculation are shown together with typical inelastic spectra in figure 1.

Figure 2 shows the integrated intensity of the paramagnetic scattering around the (0, 0, 1) Bragg point extracted form the fits. Interestingly, it can be seen that the antiferromagnetic fluctuations disappear above $T = 235$ K, which corresponds to the charge-ordering temperature $T_{CO}$. Below $T_{CO}$ we measured only a few temperature points. Figure 2 shows that the correlation length of the antiferromagnetic fluctuation increases. Actually, $\kappa(T)$ can be also fitted like $\kappa(T) = 0.03 \times (T - T^*)^{0.5}$, with $T^* = 161 \pm 3$ K, roughly indicating a mean field behaviour. However, the precise determination of $T_N = T^*$ or the critical exponent would require more points in the vicinity of $T_N$. Last, as shown in figure 3, the $q$-dependence of the damping of the antiferromagnetic fluctuations is the same at all the measured temperatures. The fit of all points including all temperature gives the $\Gamma(q) = 8.0(\pm 0.2)q^{1.5\pm0.05}$ dependence. We obtain the same critical exponent, but with higher error bars, when we fit individual temperatures separately. This critical exponent $\nu_{AF} = 1.5$ shows that the antiferromagnetic fluctuations in $Pr_{0.65}Ca_{0.35}MnO_3$ behave in a similar way as in prototype three-dimensional Heisenberg antiferromagnets like $RbMnF_3$ [20].

### *3.2. Ferromagnetic fluctuations*

Typical inelastic scans measured around the Brillouin zone centre $\vec{\tau} = (0, 0, 2)$ are shown in figure 4. As expected, the intensity of the paramagnetic fluctuations decreases and the line width increases as a function of momentum transfer $\mathbf{q}$. For each measured temperature, (below and above $T_{CO}$ but above $T_N$) the same qualitative $q$-dependence was observed.

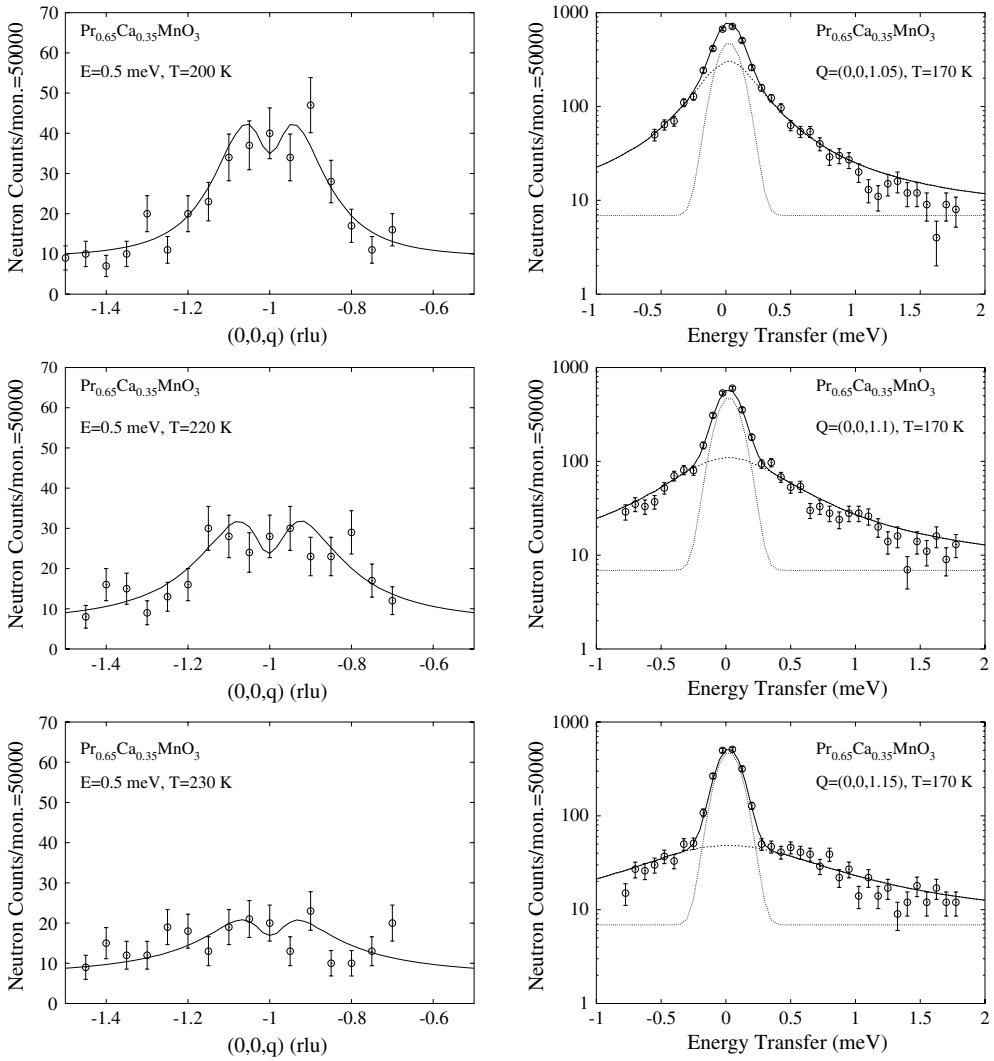


**Figure 1.** Fit of the antiferromagnetic fluctuations using equations (1)–(3). The dotted, dashed and solid lines represent the incoherent, paramagnetic and total scattering, respectively. The data are normalized to 50 000 monitor counts. Left: constant-energy scan around the AF Bragg position in $Pr_{0.65}Ca_{0.35}MnO_3$ at $T = 200$, 220 and 230 K, respectively. Right: constant-$q$ scan in $Pr_{0.65}Ca_{0.35}MnO_3$ at $T = 170$ K.

From the constant-$q$ scans shown in figure 4 it can be observed that $\kappa$ remains constant in the temperature range $200 < T < 290$ K. This shows that the correlation length $\xi$ does not depend on $T$. We find that for the ferromagnetic fluctuations $\kappa \sim 0.25$ (rlu), which corresponds to correlations between spins over a range of 3–4 lattice units only. Then we analysed the energy scans individually keeping the value of $\kappa$, as obtained from constant-energy scans, fixed. This allowed us to extract $\Gamma(\mathbf{q})$ as a function of momentum transfer. In a second step we fitted all the scans together, leaving the parameters in equation (1) free. We found that both procedures yielded similar values for $C\chi(0)$, $\kappa$ and $\Gamma(\mathbf{q})$.

The temperature dependence of the damping of the fluctuation $\Gamma(\mathbf{q}) = \gamma q^z$ obtained from such a fit to the data is tabulated in table 1, for different temperatures. Because of the large

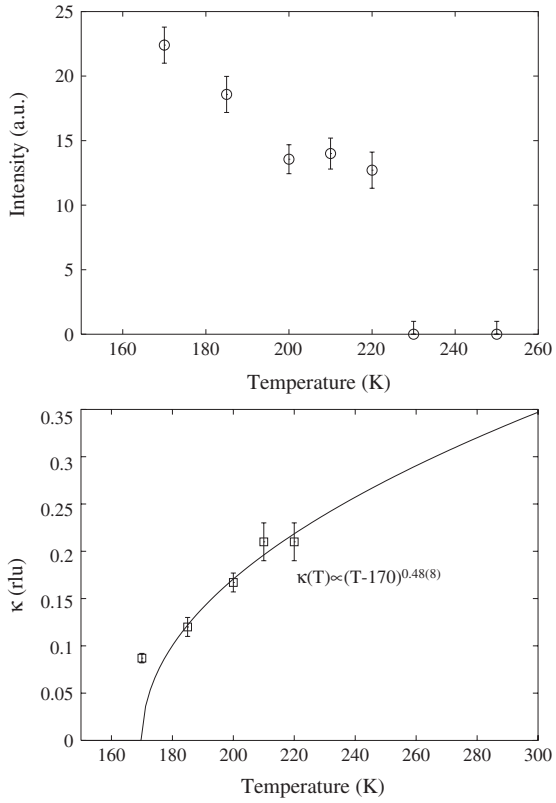


**Figure 2.** Temperature dependence of the antiferromagnetic fluctuations in $Pr_{0.65}Ca_{0.35}MnO_3$. Top: evolution of the intensity $C\chi(0)$ of the paramagnetic scattering around the antiferromagnetic position. Bottom: evolution of the inverse correlation length.

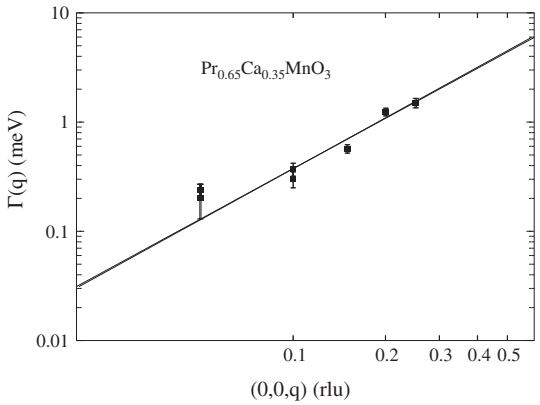


**Figure 3.** Energy damping $\Gamma(\mathbf{q})$ versus $\mathbf{q}$ at several temperatures of the antiferromagnetic fluctuations in $Pr_{0.65}Ca_{0.35}MnO_3$. The solid line is a fit to the power law $\Gamma(\mathbf{q}) = \gamma q^z$.

correlation between the damping coefficient $\gamma$ and the critical exponent $z$, the uncertainty of the two parameters is rather large. However, as shown in figure 5, no particular dependence of both parameters is observed when the temperature is varied through $T_{CO}$. We obtain for

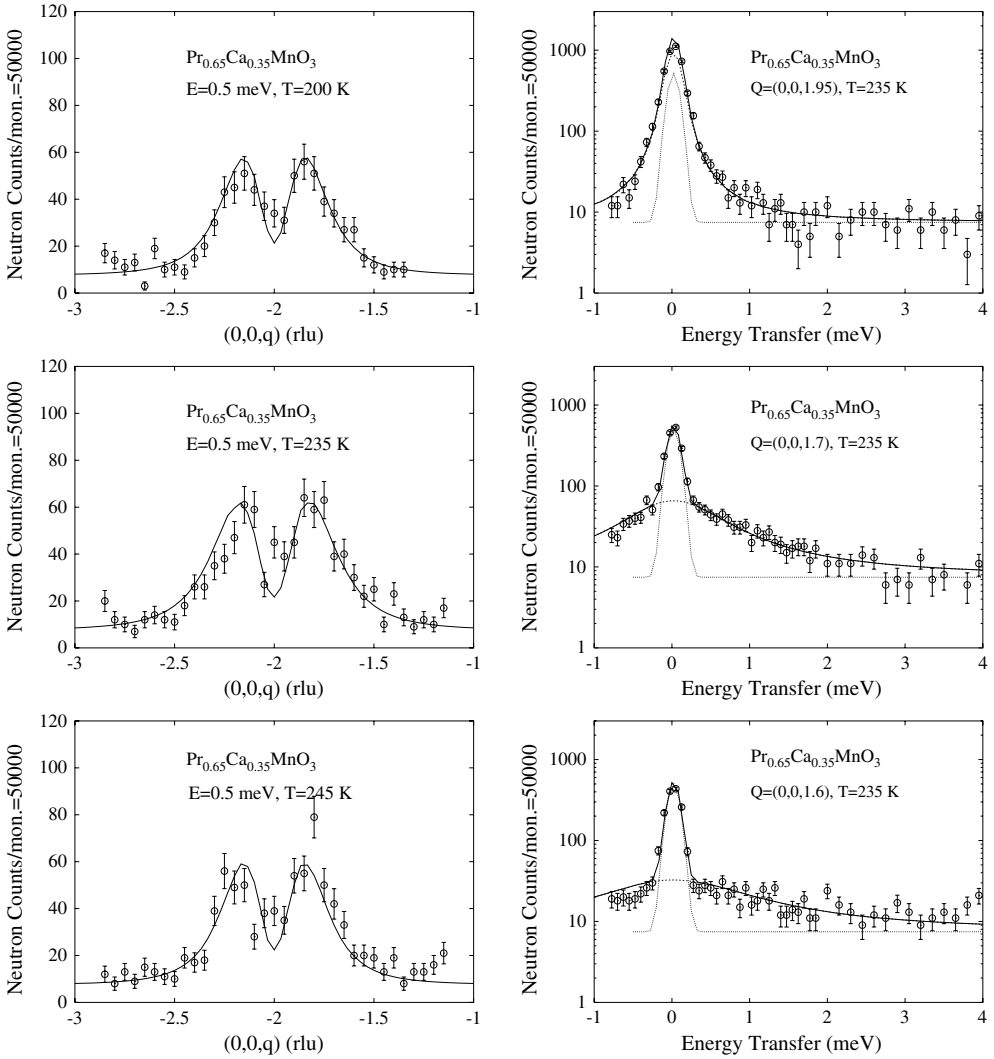


**Figure 4.** Fit of the ferromagnetic fluctuations using equations (1)–(3). The dotted, dashed and solid lines represent the incoherent, paramagnetic and total scattering, respectively. The data are normalized to 50 000 monitor counts. Left: constant-energy scan around the F Bragg position in $Pr_{0.65}Ca_{0.35}MnO_3$ at $T = 200$, 220 and 230 K, respectively. Right: constant-$q$ scan in $Pr_{0.65}Ca_{0.35}MnO_3$ at $T = 235$ K.

$Pr_{0.65}Ca_{0.35}MnO_3$ the average values $\langle\gamma\rangle = 11.4(1)$ meV/rlu$^2$ and $\langle z\rangle = 2.09 \pm 0.05$ close to the value $z = 2$ that is expected from scaling dynamics for an isotropic ferromagnet [18].

Last, we measured the temperature behaviour of the static susceptibility $\chi(\mathbf{q} \approx 0, T)$. The results are similar to that obtained by Kajimoto [19]: $\chi(\mathbf{q} \approx 0, T)$ increases on lowering the temperature toward the charge ordering temperature, but shows a sudden decrease below $T_{CO}$, as shown in figure 6. This indicates that the changes observed in the spectrum of paramagnetic fluctuations at $T_{CO}$, the appearance of antiferromagnetic fluctuations and the temperature dependence of the static susceptibility of the ferromagnetic fluctuations are related.

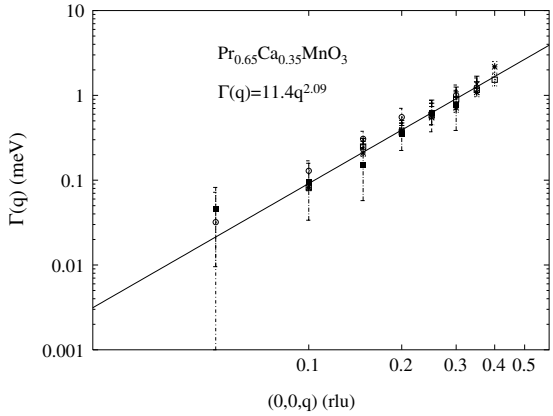


**Figure 5.** Damping of the ferromagnetic fluctuations $\Gamma(\mathbf{q})$ for $T = 200$, 215, 235, 240, 245 and 290 K, respectively. The line is a fit to the data using a power law.

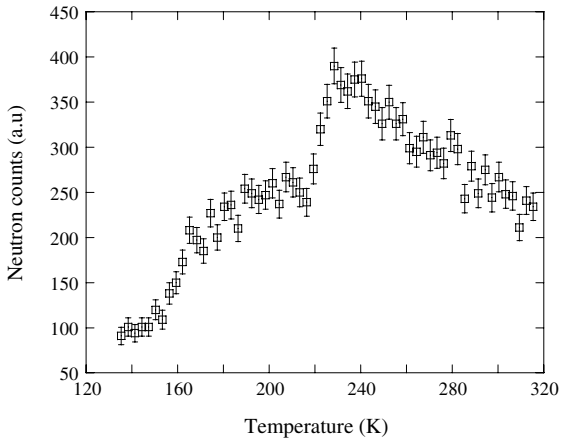


**Figure 6.** Temperature dependence of neutron intensity measured at (0,0,1.95) and $\hbar\omega = 0$ meV.

**Table 1.** Unconstrained fit of the parameters of equation (3) characterizing the ferromagnetic fluctuations of $Pr_{0.65}Ca_{0.35}MnO_3$.

| $T$ (K) | $\gamma$ (meV/rlu$^2$) | $z$ | $C\chi$ | $\kappa$ |
|---|---|---|---|---|
| 200 | 17.44(4.62) | 2.24(0.17) | 708(35) | 0.29(0.02) |
| 235 | 10.21(2.25) | 2.08(0.14) | 635(57) | 0.24(0.02) |
| 240 | 10.90(2.28) | 2.09(0.13) | 780(69) | 0.29(0.02) |
| 245 | 14.56(2.60) | 2.19(0.11) | 671(55) | 0.26(0.02) |
| 290[a] | 9.33(2.62) | 1.83(0.17) | | |

[a] This temperature was measured on another crystal, where only constant-$q$ scans were measured. For that $\kappa$ was fixed to 0.25, and we do not give $C\chi$, since it does not correspond to the other measurements.

## 4. Discussion and conclusion

We have analysed the paramagnetic fluctuations in $Pr_{0.65}Ca_{0.35}MnO_3$ around the ferromagnetic and antiferromagnetic positions. We found that the critical exponent $z$ of the antiferromagnetic

component that appears below $T_{CO}$ follows the expectations of dynamical scaling theory for a 3D Heisenberg antiferromagnet.

We confirm the unconventional nature of the ferromagnetic fluctuations [19, 22], whose characteristics are very similar to the central peak component observed in the paramagnetic insulating state of $La_{0.66}Ca_{0.33}MnO_3$, which is a ferromagnetic metal below $T_C$ [22]. In $Pr_{0.65}Ca_{0.35}MnO_3$, the correlation length $\kappa^{-1}$ of the fluctuations remain short-ranged at all the temperatures studied, and do not show any critical behaviour on crossing $T_{CO}$. This implies the existence of nanoscale regions wherein which the De Gennes double exchange mechanism is active above and below the charge-ordering transition at $T_{CO}$.

Additionally to previous results, we have extracted the temperature dependence of other dynamical parameters: like in $La_{0.66}Ca_{0.33}MnO_3$ [22], we infer a dynamical critical exponent of $z \approx 2$, which agrees well the exponent predicted by the dynamical scaling theory for a Heisenberg ferromagnet. However, we also find that the parameters $\gamma$ and $\kappa$ characterizing respectively the energy or $q$-dependence of these fluctuations are insensitive to $T_{CO}$, which contrasts with the strong temperature dependence of the static susceptibility $\chi(\mathbf{q} \approx 0, T)$ (figure 6) already reported before by Kajimoto [19]. It must be concluded that there exist a cutoff value $\mathbf{q}_c$, below and above which the ferromagnetic fluctuations are actually probing phenomena that are differently sensitive to charge ordering.

In order to qualitatively understand this, we point to the first refinement charge-ordered superstructure of a $Pr_{0.60}Ca_{0.40}MnO_3$ from single crystal neutron diffraction, which recently suggested an alternative structural model for half-doped manganites [13] that contradicts the ionic charge-ordering model. This structural model served as a basis for introducing a novel, so-called Zener polaron (ZP) ordering picture of the charge-ordering phenomenon. The ZP formation is invoked from the recent work of Goodenough (see [14] for a review), who calls for the need to distinguish between two different forms of double exchange in manganites: that of de Gennes [5, 6], and that of Zener [7]. De Genes considered double exchange as a mechanism inducing the *delocalization* of the $e_g$ charges in a spin-polarized conduction band [5, 6]. However, Goodenough recalls that Zener originally addressed the transfer of single $e_g$ charges at the Mn–O–Mn level [7], and further suggests that $e_g$ charges coupled to oxygen vibrations can transmit a DE interaction restricted to this molecular level. This defines a local form of the DE mechanism inducing the *localization* of the $e_g$ electrons onto pre-formed ferromagnetic Mn pairs, the ZPs.

Zhou and Goodenough evidenced ZP formation in several manganite compounds lying exactly at the borderline between localized and itinerant behaviour like $La_{7/8}Sr_{1/8}MnO_3$, or the colossal magneto-resistive $(La_{1-z}Nd_z)_{0.7}Ca_{0.3}MnO_3$ manganite ferromagnets [15]. They did not anticipate that ZPs could be also the building unit of the insulating charge-ordered $Ln_{1/2}Ca_{1/2}MnO_3$ (Ln: Pr, La) compounds, as interpreted by Daoud *et al* [13]. The overall magnetism/structure correlation in the latter compounds can be redrawn with super-exchange interactions coupling ZPs instead of ordered $Mn^{3+}/Mn^{4+}$ ions [16, 17].

In particular, the ZP ordering picture qualitatively explains why all the charge-ordered manganites show an anomaly of the macroscopic spin susceptibility $\chi(T)$ at $T_{CO}$. In a few charge-ordered compounds, which have a wide temperature range between $T_{CO}$ and $T_N$ such as $Y_{1/2}Ca_{1/2}MnO_3$ ($T_{CO}$–$T_N \sim 170$ K) or $Bi_{1-x}Sr_xMnO_3$ ($T_{CO}$–$T_N \sim 460$ K), $\chi(T)$ displays an asymptotic Curie–Weiss behaviour in the charge-ordered paramagnetic state, from which an effective paramagnetic moment can be extracted. In such cases, the experimental value is always higher than the effective moment above $T_{CO}$, and it always agrees quantitatively with the ZP ordering picture [13, 21]. Here, the temperature dependence of the static susceptibility $\chi(\mathbf{q} \approx 0, T)$ shown in figure 6, which is the same as that of $\chi(T)$, is most probably associated with ZP polaron formation at $T_{CO}$. In $Pr_{0.65}Ca_{0.35}MnO_3$, the charge-ordered phase is, however,

only visible in a small temperature range ($T_{CO}$–$T_N \sim 50$ K) and the static susceptibility additionally contains a contribution from the magnetic Pr ions. This prevents the unambiguous extraction of an effective paramagnetic moment.

In the light of this, we suggest that the dual nature of the ferromagnetic fluctuations could relate to the two types of Zener and De Gennes double exchange mechanisms, which would coexist in the whole studied temperature range $T_N < T < 300$ K. At $T_{CO}$, the anomalous behaviour of the static susceptibility $q \sim 0$ can be qualitatively explained by charge ordering viewed as a ZP ordering phenomenon [13]: this ordering of super-exchange coupled ferromagnetic Mn pairs corollary explains the appearance of the antiferromagnetic correlations. On the other hand for $q \neq 0$, short-ranged ferromagnetic fluctuations are observed, which have temperature-independent characteristics across $T_{CO}$: their energy damping indicates a spin-diffusion process originating from a conventional De Gennes double exchange [22] mechanism, which acts into nanoscale regions embedded in the insulating matrix. The latter mechanism survives below $T_{CO}$, and it is only suppressed by the antiferromagnetic ordering. As we can guess from figure 5, more precise studies of the low-$q$ ($q < 0.1$ rlu) dynamical susceptibility are needed to make a better distinction between the two ferromagnetic components.

## Acknowledgment

This work was performed at the spallation neutron source SINQ, Paul Scherrer Institut, Villigen (Switzerland).

## References

[1] Jin S *et al* 1994 *Science* **264** 413
[2] Urushibara A, Moritomo Y, Arima T, Asamitsu A, Kido G and Tokura Y 1995 *Phys. Rev.* B **54** 14103
[3] Wollan E O and Koehler W C 1955 *Phys. Rev.* **100** 545
[4] Schiffer P *et al* 1995 *Phys. Rev. Lett.* **75** 3336
[5] Anderson P W and Hasegawa H 1955 *Phys. Rev.* **100** 675
[6] de Gennes P-G 1960 *Phys. Rev.* **118** 141
[7] Zener C 1951 *Phys. Rev.* **82** 403
[8] Goodenough J B 1955 *Phys. Rev.* **100** 564
[9] Radaelli P G, Cox D E, Marezio M and Cheong S-W 1997 *Phys. Rev.* B **55** 3015
[10] Jirak Z, Krupicka S, Simsa Z, Dlouha M and Vratislav S 1985 *J. Magn. Magn. Mater.* **53** 153
[11] Tokunaga M, Miura N, Tomioka Y and Tokura Y 1998 *Phys. Rev.* B **57** 5259
[12] Cox D E, Radaelli P G, Marezio M and Cheong S-W 1998 *Phys. Rev.* B **57** 3305
[13] Daoud-Aladine A, Rodríguez-Carvajal J, Pinsard-Gaudart L, Fernández-Diaz M-T and Revcolevschi A 2002 *Phys. Rev. Lett.* **89** 097205
[14] Goodenough J B 2001 *Localized to Itinerant Transitions in Perovskite Oxides. Structure and Bonding* ed J B Goodenough and S Copper (Berlin: Springer)
[15] Zhou J-S and Goodenough J B 2000 *Phys. Rev.* B **62** 3834–8
Zhou J-S and Goodenough J B 1998 *Phys. Rev. Lett.* **80** 2665
[16] Daoud-Aladine A, Rodríguez-Carvajal J, Pinsard-Gaudart L and Revcolevschi A 2004 *J. Magn. Magn. Mater.* **272–276** (Suppl. 1) E1387–8
[17] Zheng G and Patterson C H 2003 *Phys. Rev.* B **67** 220404
[18] Halperin B I and Hohenberg P C 1969 *Phys. Rev.* **177** 952
[19] Kajimoto R, Kakeshita T, Oohara Y, Yoshizawa H, Tomioka Y and Tokura Y 1998 *Phys. Rev.* B **58** R11837
[20] Coldea R, Cowley R A, Perring T G, McMorrow D F and Roessli B 1998 *Phys. Rev.* B **57** 5281–90
[21] Frontera C *et al* 2003 *Phys. Rev.* B **68** 134408
[22] Lynn J W, Erwin R W, Borchers J A, Huang Q, Santoro A, Peng J-L and Li Z Y 1996 *Phys. Rev. Lett.* **76** 4046